Authors' Response

We would like to thank both reviewers for their helpful comments on the manuscript. The detailed questions and suggestions helped improving the manuscript a lot.

In the following, we will answer the comments of both reviewer in one document, starting with reviewer 1. Italics indicate reviewer comments and changes to the manuscript are in blue font. Page numbers and line number reference the originally submitted manuscript.

Following the specific answers, we've attached the updated manuscript with the changes marked in color. Red indicates parts that have been removed and blue indicates parts that have been added.

Comments from Reviewer #1

My main 3 comments are that

1) it would be nice to see an example of at least one scientific application of the dataset, including retrieved liquid water path, water vapor paths, radar/lidar derived cloud properties. Figures 2 and 3 are good as it is also nice to see what the actual quicklooks look like. These also communicate that the retrieval work remains to be done. Are there any examples of retrieved physical quantities from any of the flights that could be mentioned? Or any scientific results, perhaps already published in other papers? This could be considered to fall outside the scope of the ESSD journal, and if the editor also feels that way, then so be it, but it would help increase the impact of the manuscript to show the reader why they might be interested in working with it.

Since the scope of the ESSD journal are articles on original research data sets. We focus in this manuscript only on the level 1 data that is quality controlled and published along with the manuscript. However, retrieval development with this data has been already started and we agree that an example of the possible products might be very helpful for the user. We therefore included an additional figure (Fig. 3 in the updated manuscript) from the publication about the developed retrievals for liquid water path (Jacob, et al., 2019) to demonstrate the potential of the data. We extended the text in the manuscript to include this:

In summary, the combination of measurements from different channels can be used to derive the integrated water vapor and liquid water path (Schnitt et al., 2017; Jacob et al., 2019), coarse resolution temperature and moisture profiles as well as information on ice and snow occurrence. An example of retrieved liquid water path and rain water path is shown in Fig. 3 to demonstrate the potential of the HAMP measurements. This scene from the NARVAL1 campaign shows the time series of the retrieved quantities together with radar reflectivity measurements. The retrieval algorithm is described in depth in Jacob et al. (2019).

2) My second comment is that the manuscript contains many small grammatical inconsistencies. These merely reflect that the authors are not native English speakers and the meaning is generally clear, but if a native English speaker could be found to read through the manuscript and improve the English, that would be worth doing.

We thank the reviewer for their comments and suggestions about the wording of the manuscript. We asked a native speaker to review the manuscript to improve the language and applied their comments to our manuscript.

3) My third comment is that the description of the Vaisala dropsondes, "RD94" on p. 6, doesn't mean anything to mean. Some description and a reference to their performance would be nice. Is a

correction incorporated for a solar radiation bias, as is done for research grade radiosondes in the US? Are there any issues for the user to be aware of?

We have extended the description of the dropsondes in the manuscript by values of measurement accuracies and the relevant citations.

The extended section about the dropsondes now reads:
Vaisala RD94 dropsondes (Busen, 2012) were deployed in all campaigns using the Airborne Vertical Atmospheric Profiling System (AVAPS, Hock and Franklin, 1999). Wang et al. (2015) and Vaisala (2017) report that the measurement accuracy of these sondes for pressure is 0.4 hPa, temperature is 0.2 ºC and relative humidity is 2%. The accuracy of horizontal wind speed measurements is estimated to be 0.1 m s^{-1}.

We are not aware of any applications of corrections for solar radiation bias. We would however argue that this effect would be almost negligible in the case of this data set: The dropsondes were mainly dropped from around 8 km altitude. Average descent rate of dropsondes through the troposphere is about 10 m/s while average ascent rate of radiosondes in the troposphere is around 5 m/s. The time the dropsondes are influenced by solar radiation is therefore much shorter than for radiosondes.

According to the solar radiation correction table for RS92 radiosondes on the Vaisala webpage (https://my.vaisala.net/en/meteorology/products/soundingsystemsandradiosondes/soundingdatacontinuity/RS92-Data-Continuity/Pages/solarradiationcorrectiontable.aspx, accessed on 23. May 2019), the correction values for the lower troposphere, where the majority of the dropsondes have been dropped, are rather small: between 0.04 ºC for low solar angles and 0.14 ºC for higher angles. This is below the reported accuracy of the temperature sensor. In our opinion, this, together with the faster descends of the dropsondes, this justifies not correcting the temperature measurements for solar radiation biases.

Minor comments:

page 1, line 21: "the full atmospheric column...." this depends on the frequency, would be worth stating.

We have added this to the text the sentence now reads:
Microwave frequencies are especially suited for cloud and precipitation remote sensing as they can, depending on the individual frequencies, penetrate the full atmospheric column in contrast to solar and infrared remote sensing which are mainly limited to thin clouds and cloud top regions.

page 2, line 4-5: "12 dBZ....typical for light precip.." is confusing. How about : "12 dBZ, more suited for the detection of heavier precipitation, and less so for characterizing shallow convection."

Thank you for this suggestion. We have changed the sentence to:
Passive microwave satellite instruments have footprints of several tens of kilometers (Elsaesser et al., 2017) while active microwave instruments are confined to narrow scan regions, limited vertical resolution and sensitivity, i.e. the Global Precipitation Mission (GPM) 35 GHz radar has a minimum detectable signal of 12 dBZ (Skofronick-Jackson et al., 2013), more suited for the detection of heavier precipitation, and less so for characterizing shallow convection.

p. 2, line 6: to -> with
p. 2 line 22: put "The" before "Center"
line 24: put 'was' before 'again'

We have corrected the points mentioned above.

lines 27,28: the verb tenses are not consistent.

We have changed the sentence to:

HAMP observations from NAWDEX give insight into convective clouds and their surroundings in the frontal regions and warm sector of mid-latitude cyclones.

p. 3, line 16: "collocating tracks": the word 'collocating' is used a lot within the manuscript. This is the first instance. At first I was not sure what the authors meant, it is not a typical usage. Perhaps rephrase as "and to evaluate satellite observations through flying underneath the satellite, along the projected satellite track near the satellite overpass time". Once this is clearly defined the continued use of 'collocated' will be clear I think.

We thank the reviewer for pointing this out. We changed the first mention of collocation to the following sentences:

Additionally, the focus of this campaign was to assess the representativeness of ground-based measurements on Barbados (Stevens et al., 2016) for a broader trade wind region over the tropical Atlantic and to evaluate satellite observations on collocated tracks (Klepp et al., 2014; Stevens et al., 2016). This has been done by flying underneath the satellite, along the projected satellite track near the satellite overpass time.

line 28: were -> was
p. 4, line 5: in -> for a
line 6: always precede "Center" with a "The".
p.5, line 10: with -> at, in -> while

We have corrected the points mentioned above.

p.6 line 20: How can the median drift in the upper quartile (of what?) exceed the total median drift length? was there always wind shear present? I couldn't quite follow this sentence.

We thank the reviewer for pointing out, that this sentence was hard to follow. The statement should be about the distribution of horizontal drift distances from all dropsonde profiles. The median of all horizontal drift distances is 3.8 km, the lower quartile of horizontal drift distances is 2.3 km and the upper quartile of these is 10.8 km. We have rewritten the sentence to the following:

The length of the horizontal drift distance varied substantially from drop to drop. The median of the horizontal drift distances for all dropsonde measurements was 3.8 km, while the upper and lower quartile of horizontal drift distances was 10.8 km and 2.3 km, respectively.

line 23: were -> where
line 24: replace "and be able to release sondes" with ", where the sondes could be released." line 28: include 'lower tropospheric' before 'profile'
p.7 lines 2-3 can be removed, this has already been stated.

We have corrected the points mentioned above.

over all the data description is okay, but the quicklooks, especially of the Tb, do not provide much information. An example of, e.g., the ability to retrieve a temperature profile, with a comparison to a dropsonde, would be nice.

We completely agree, that quicklooks from brightness temperatures are hard to interpret. As we mentioned in the beginning, we focus this manuscript on the description of the original data set and their quality control procedures. To give a better insight into the potential of the data, we added Figure 3 to the manuscript which shows retrieved liquid water path and rain water path in comparison with radar reflectivity measurements from Jacob et al. (2019).

A lot of the evaluation of the data and retrieval development for profiles is still ongoing work. Unfortunately, we can not give an example for this as this has not been finished yet. But we would still like to publish the data set and make it available for the community, to give others the opportunity to use this data set for developing and testing their own retrievals.

p.8 line 7: add "of clear skies" after "profiles"
line 25: rewrite sentence as "The erroneous time stamps were reconstructed where possible" line 29-30: rewrite the 2nd phrase to remove the passive voice. 'appeared to be' -> are. remove 'about'
line 31: add 'angles' after 'bank'

We have corrected the points mentioned above.

p9 line 1: 'They' -> The comparison

We have rewritten the sentence:
Ewald et al. (2018) concluded that the resulting bias of 7.6 dBZ originated from differences in software configuration and instrument calibration.

line 22: add 'the' before 'height'
p. 10 line 9: corresponding -> correspond

We have corrected the points mentioned above.

p. 11 line 9: has-> have

We did not find the word "has" on page 11, line 9. We did, however, find that the word "has" in line 14 on the same page should be changed to "have" to be consistent in the use of the word "data" as plural throughout the manuscript. We changed an additional instance of this on page 9, line 9.

Table 1: 'shallow trade wind convection' occurs within every Flight characteristics. consider putting this in the table caption and restricting the characteristics to more differentiating features.

We thank the reviewer for this suggestion. The table caption now reads:
List of NARVAL-South flights. All flights include observations of shallow trad wind convection. Additional flight characteristics are listed in the last column.

Table 5: "BAHAMAS" should be defined. not everyone will read the main text.

We added the explanation of the synonym (BAHAMAS: BAsic HALO Measurement And Sensor system) as a footnote to the table.

Comments from Reviewer #2

Although publishing this data set is important, I would urge the authors to consider additional outreach. For NWP, they might contact the NWP satellite applications facility (https://www.nwpsaf.eu/site/) advertising this data set for 1-dimensional radiance assimilation testing with their microwave imaging processing package (https://www.nwpsaf.eu/site/software/mwipp/). For additional outreach to the climate community, the authors may try contacting the Copernicus Climate Change Service hosted by ECMWF (https://climate.copernicus.eu/) and the CMIP group in the USA at PCMDI (https://pcmdi.llnl.gov/index.html) as well as the Earth System Grid Fed- eration https://esgf.llnl.gov/). (I know that co-author Stevens has been active in this area as has Prof. Bony who appears to be a lead organiser of the Field campaign.

We thank the reviewer for pointing out the possible applications in the NWP and climate community. This is in part the reason why we decided to publish the data via the CERA database. The database assures good findability of the datasets by requiring detailed metadata for all published dataset. These metadata are then indexed by different other databases for a broader reach across the communities. For example, the CERA database is part of the Global Information System Centres (GISC) via the German Weather service. The data is also findable via the EUDAT collaborative data infrastructure thanks to the standard of the CERA database. The published HAMP dataset is therefore already accessible quite well. We will however keep this in mind and check if this setup is sufficient or if other steps might be necessary to advertise the data set to an even broader community.

It would be helpful for the authors to identify a potential physical mechanism for the application of the global bias identified in section 5.1 between the forward radiative transfer Tb computed from the profile data and the microwave measurements. Perhaps this is still under study. Microwave observations are sometimes subject to side lobe contamination biases that can be very difficult to identify and correct. Perhaps some others can comment on exercising the data.

Unfortunately we don't have a definitive answer to this. We are aware of the fact, that our measurements are not perfect. Microwave radiometer instruments on an aircraft are unfortunately always subject to vibration and temperature changes which can influence the behavior of the instruments in an unpredictable way.

We don't think that contamination from side lobes would be a large problem, since the environment in which the measurements are conducted is usually very homogenous. And so, even if there were influences from the sides, this should be not too different from the measurements directly nadir below the aircraft.

Up until now, we can't ultimately explain this bias. We found biases in the data systematically for all flights. But even after all our analyses, uncertainties still remain and the exact reason for these differences are still unclear. We decided therefore to thoroughly identify the biases in our measurements, report on all our findings, and include the information in the data files. Our main result from this investigation is, that a calibration against at least one clear-sky dropsonde per flight is needed.

Bibliography

Jacob, M., Ament, F., Gutleben, M., Konow, H., Mech, M., Wirth, M., and Crewell, S.: Investigating the liquid water path over the tropical Atlantic with synergistic airborne measurements, Atmos. Meas. Tech. Discuss., pp. 1–27, https://doi.org/10.5194/amt-2019-18, https://www.atmos-meas-tech-discuss.net/amt-2019-18/, 2019.

A unified data set of airborne cloud remote sensing using the HALO Microwave Package (HAMP)

Heike Konow[1], Marek Jacob[2], Felix Ament[1,3], Susanne Crewell[2], Florian Ewald[4], Martin Hagen[4], Lutz Hirsch[3], Friedhelm Jansen[3], Mario Mech[2], and Bjorn Stevens[3]

[1]Universität Hamburg, Hamburg, Germany
[2]Institute for Geophysics and Meteorology, University of Cologne, Cologne, Germany
[3]Max Planck Institute for Meteorology, Hamburg, Germany
[4]German Aerospace Center DLR, Oberpfaffenhofen, Germany

Correspondence to: Heike Konow (heike.konow@uni-hamburg.de)

Abstract. Cloud properties and their environmental conditions were observed during four aircraft campaigns over the North Atlantic on 37 flights. The Halo Microwave Package (HAMP) was deployed on the German research aircraft HALO (High Altitude LOng range research aircraft) during these four campaigns. HAMP comprises microwave radiometers with 26 channels in the frequency range between 20 and 183 GHz and a 35 GHz cloud radar. The four campaigns took place between December 2013 and October 2016 out of Barbados and Iceland. Measured situations cover a wide range of conditions including the dry and wet season over the tropical Atlantic and the cold and warm sectors of mid-latitude cyclones. The data set we present here contains measurements of the radar reflectivity factor and linear depolarization ratio from cloud radar, brightness temperatures from microwave radiometers, and atmospheric profiles from dropsondes. It represents a unique combination of active and passive microwave remote sensing measurements and 525 in-situ measured dropsonde profiles. The data from these different instruments are quality controlled and unified into one common format for easy combination of data and joint analysis. The data are available from the CERA database for the four campaigns individually (https://doi.org/10.1594/WDCC/HALO_measurements_1, https://doi.org/10.1594/WDCC/HALO_measurements_2, https://doi.org/10.1594/WDCC/HALO_measurements_3, https://doi.org/10.1594/WDCC/HALO_measurements_4). This data set allows for analyses to get insight into cloud properties and the atmospheric state in remote regions over the tropical and mid-latitude Atlantic. In this paper, we describe the four campaigns, the data and the quality control applied to the data.

1 Introduction

Clouds in the planetary boundary layer over oceans have been identified as one of the largest contributors to intermodel spread in climate sensitivity (Sherwood et al., 2014) and more detailed observations are needed for model improvement (Bony et al., 2015). Modern satellites provide detailed insights into cloud structures and their microphysical characteristics with almost full coverage of the Earth. In contrast to solar and infrared remote sensing, which are mainly limited to thin clouds and cloud top regions, microwave frequencies are especially suited for cloud and precipitation remote

sensing, depending on the individual frequencies. However, most microwave satellite products are limited in resolution, coverage and sensitivity. Passive microwave satellite instruments have footprints of several tens of kilometers (Elsaesser et al., 2017), while active microwave instruments are confined to narrow scan regions, limited vertical resolution and sensitivity. For example the Global Precipitation Mission (GPM) 35 GHz radar has a minimum detectable signal of 12 dBZ (Skofronick-Jackson et al., 2013), which is more suited for the detection of heavier precipitation and less so for characterizing shallow convection. Therefore, the synergy of airborne active and passive microwave remote sensing has mostly been used for liquid and solid precipitation in the preparation and validation phase of the Global Precipitation Mission (GPM; e.g. Houze et al., 2017; Skofronick-Jackson et al., 2013). A better sensitivity with respect to non-precipitating clouds is achieved by the CloudSat radar, which has a minimum detectable signal of about -27 dBZ (Stephens et al., 2002). However, the vertical pulse resolution of about 500 m becomes problematic for boundary layer clouds.

Ground-based remote sensing stations can provide measurements with high temporal and vertical resolution but are limited to few locations that are almost exclusively on land. Airborne remote sensing bridges this gap between coarse satellite observations and stationary ground-based measurements. The HALO aircraft (High Altitude LOng range research aircraft, Krautstrunk and Giez, 2012; Wendisch et al., 2016) with its long range, high ceiling and the possibility for carrying a heavy payload is a great platform to explore clouds in maritime conditions over the ocean with highly resolved measurements. The HALO Microwave Instrument Package (HAMP, Mech et al., 2014) has been developed to allow for in-depth remote sensing of clouds and their microphysical properties. It consists of a 35 GHz cloud radar and a 26 channel microwave radiometer covering a spectral range from 20 to 183 GHz.

In this article, data sets from four campaigns performed in different climate regimes are presented. The first campaign, NARVAL1 (Next-generation Aircraft Remote sensing for VALidation Studies), consisted of two sub-campaigns: NARVAL-South and NARVAL-North. In December 2013, NARVAL-South focused on observations of shallow convection in the trade wind region of the eastern tropical Atlantic during the dry season and consisted of eight research flights out of Barbados (Fig. 1 (a)). During NARVAL-North in January 2014, post-frontal regimes over the extratropical North Atlantic were observed with seven research flights. The center of operations was Keflavik, Iceland (Fig. 1 (b)). An overview of all NARVAL1 flights and measurements is provided by Klepp et al. (2014). NARVAL2 succeeded this first demonstrator mission in August 2016. During this campaign, HALO was again deployed to Barbados (Fig. 1 (c)). NARVAL2 measurements complement the NARVAL-South measurements with observations of the atmosphere over the tropical Atlantic during the wet season (Stevens et al., 2019). Directly following the NARVAL2 mission, the same HALO payload was flown during the NAWDEX (North Atlantic Waveguide and Downstream Impact Experiment) campaign (Schäfler et al., 2018). Here, HALO was again deployed to Keflavik, Iceland, for five weeks in September and October 2016 (Fig. 1 (d)). HAMP observations from NAWDEX give insight into convective clouds and their surroundings in the frontal regions and warm sector of mid-latitude cyclones. In this paper, a unified data set comprising HAMP measurement data from the four campaigns described above is presented and made available.

The measurements were rigorously quality controlled to ensure temporal collocation of all instruments and to remove erroneous measurements. Additionally, a quality flag has been added to the data sets to communicate the quality of each data point. The data have been regridded onto a unified grid for easily combined analyses of the measurements. The HAMP data, together with dropsonde measurements, provide insights into cloud geometry, hydrometeors, vertically integrated humidity and thermodynamic profiles.

Section 2 gives specific information about the four campaigns. A detailed description of the aircraft and instruments is given in Sect. 3. The data set is described in Sect. 4, and the quality control is outlined in Sect. 5. Information about how the data can be accessed is given in Sect. 6.

2 Campaigns with NARVAL payload

So far, the HAMP instrument suite has been part of the HALO payload (refered to as the NARVAL payload) during four campaigns: NARVAL1 (with sub-campaigns NARVAL-South and NARVAL-North), NARVAL2 and NAWDEX. Two campaigns focused on the observation of clouds and convection over the tropical Atlantic during the dry season (NARVAL-South) and wet season (NARVAL2). The goals of the other two campaigns were the observation of clouds and convection associated with the cold sector (NARVAL-North) and warm sector (NAWDEX) of mid-latitude cyclones. During all campaigns, all transfer flights were also research flights with full measurements. The individual campaigns are described in more detail below.

2.1 NARVAL-South

The first NARVAL campaign (NARVAL-South) took place between 10 December 2013 and 22 December 2013. This campaign and the campaign that followed directly after, NARVAL-North, were first and foremost planned as a demonstrator mission to assess the capabilities of HALO and HAMP to work as an airborne cloud remote sensing platform. Additionally, the focus of this campaign was to assess the representativeness of ground-based measurements on Barbados (Stevens et al., 2016) for a broader trade wind region over the tropical Atlantic and to evaluate satellite observations on collocated tracks (Klepp et al., 2014; Stevens et al., 2016). This has been done by flying underneath the satellite, along the projected satellite track near the satellite overpass time. In total, eight flights amounting to about 67 flight hours were conducted. Of the eight flights, four flights were cross-Atlantic transects during transfers between Oberpfaffenhofen, Germany (OBF) and Grantley Adams International Airport, Barbados (BGI), and four were local flights over the tropical North Atlantic east (and upwind) of Barbados. The overall flight time for individual flights was around 10 hours for transatlantic flights and around 7 hours for local flights. Target areas of this campaign were the trade wind region east of Barbados as well as cross-Atlantic transects. The synoptic situation was relatively constant from flight to flight. Therefore, flight planning was done mainly in the interest of gathering statistically sound data and to compare with satellite data. A-Train collocations were achieved during seven flights. All flights and their aims are listed in Table 1, and flight tracks are shown in Fig. 1 (a).

2.2 NARVAL-North

Following directly after the first campaign, NARVAL-North took place from 07 January 2014 to 22 January 2014. ~~Center~~ The center of operation was at Keflavik International Airport, Iceland (KEF). During this campaign, seven flights were conducted, overall amounting to 46 flight hours. The target area ~~were~~ was the extra-tropical North Atlantic south and south-west of

5 Iceland. The aim of NARVAL-North was to analyze post-frontal convective regimes of mid-latitude cyclones over the extra-tropical North Atlantic and to investigate the accuracy of existing satellite precipitation climatologies (Klepp et al., 2014). Flight planning was done taking into account current synoptic situations. The flights mainly sampled the cold sector of mid-latitude cyclones as well as some occlusions. A-Train collocations were achieved during four flights. Figure 1 (b) shows the flight tracks of NARVAL-North and in Table 2 all flights and their aims are listed.

10 ## 2.3 NARVAL2

NARVAL2 followed up on NARVAL-South with a stronger focus on the local region around Barbados and over the tropical Atlantic between 8 August 2016 and 30 August 2016. Ten research flights were flown ~~in~~ for a total of about 84 flight hours (Table 3) with different flight tracks (Fig. 1 (c)). ~~Center~~ The center of operation was again BGI on Barbados. A-Train collocations were achieved during five flights ~~,~~ as well as collocations with the satellites GPM (Global Precipitation Measurement) and

15 Megha-Tropiques. The aim of the campaign was to assess the interaction between large-scale dynamics and the evolution of convective systems over the tropical Atlantic ~~(Ste)~~ (Stevens et al., 2019). Of the 10 flights during this campaign, 2 flights were transfers to and from Barbados. The remaining flights took place over the tropical North Atlantic east and south-east of Barbados. Three of these flights focused on clouds in and associated with the Intertropical Convergence Zone (ITCZ). The other five flights took place further north and mainly over shallow convection. Two flights focused on the surrounding atmosphere

20 of Hurricane Gaston (2016). However, due to instrument failure, no radar measurements are available from these two flights. A special flight pattern, i.e. circles with a radius of about 110 km with frequent dropsonde launches, was performed in order to measure the large-scale vertical motion ~~(?)~~ (Bony and Stevens, 2019) on six flights.

2.4 NAWDEX

The fourth campaign of this set, NAWDEX, took place from 17 September 2016 until 18 October 2016. ~~13~~ Thirteen flights

25 amounted to about 96 flight hours. During this campaign, HALO, along with other research aircraft, was stationed at KEF on Iceland. Figure 1 (d) shows the flight tracks of NAWDEX. A-Train collocation was achieved during one flight. Of the 13 flights ~~of~~ during this campaign, ~~2~~ two were transfers to and from Keflavik. The main target of the flights during this campaign ~~were~~ was the clouds associated with the warm conveyor belt of mid-latitude cyclones (Schäfler et al., 2018). Flight planning was done taking into account current synoptic situations. In Table 4, all flights and their aims are listed. The flights mainly sampled

30 the warm sector and frontal systems of mid-latitude cyclones.

3 Aircraft and instrumentation

Instruments described in this paper were part of the NARVAL payload on board the German research aircraft HALO (High Altitude LOng range research aircraft). The aircraft, the HAMP instruments, and the dropsondes are described in the following sections.

3.1 The HALO aircraft

The HALO aircraft is a Gulfstream G550 with a ceiling altitude up to 15 km and long endurance of up to 10 h (Krautstrunk and Giez, 2012; Wendisch et al., 2016). HALO's capabilities of high ceiling and long range enables researchers to cover a wide variety of atmospheric conditions during a single flight and to fly above the main airline traffic and most cloud systems. Thus, measurements on board HALO often provide a view of at least a large part of or even the entire troposphere through measurements. The median flight altitude was 13.1 km for the NARVAL-South campaign and 7.8 km during NARVAL-North, taking into account the lower tropopause height of the target region in winter and flight restrictions. During NARVAL2, the median flight altitude was 9.7 km and during NAWDEX 12.4 km. The lower altitudes during NARVAL2 were flown to accommodate for the fact that dropsondes were launched in quick succession during some of these flights (see Sect. 3.2.3).

The HALO aircraft is equipped with the BAsic HALO Measurement And Sensor system (BAHAMAS). This instrument system provides data about the aircraft's location and attitude (position, altitude, heading, roll and pitch angle) and atmospheric measurements at aircraft level (e.g. temperature, humidity, pressure) (Krautstrunk and Giez, 2012). During the first two campaigns, data were sampled at 1 Hz, while in 2016, 100 Hz data were also available. In this data set, however, the 1 Hz data are provided for all flights, since these correspond best to the sampling rates of the other instruments. Measurements of aircraft location (latitude, longitude, altitude above WGS84 ellipsoid) and attitude (angles of roll, pitch and heading) are provided in this data set. Note that most measurements were performed in straight legs or large circles with only 6.72 % of the measurements having a roll angle of more than 5°.

The median speed above ground was 224 m s^{-1}, and therefore, measurements with a resolution of 1 s roughly represent a distance of about 200 m. Typically, it took 35 minutes to reach flight level after takeoff and 30 minutes for the final descent.

3.2 Instrument description

The HALO Microwave Package (HAMP, Mech et al., 2014) comprises microwave radiometers with 26 channels in the range between 20 and 183 GHz and a 35 GHz cloud radar. The radiometer modules and radar antenna are mounted below the fuselage inside the belly pod (see Fig. 1 of Mech et al. (2014)) with a nadir viewing direction. Mech et al. (2014) illustrate the sensitivity of the different measurements with respect to hydrometeors. Besides the HAMP data, profiles from dropsonde measurements and auxiliary data from the aircraft's basic data system are also included in the published data set described here. The specifications of these instruments are listed in Table 5 and are described in the following sections.

3.2.1 Microwave radiometers

The HAMP microwave radiometers were custom-manufactured by Radiometer Physics GmbH (RPG, Meckenheim, Germany). They comprise five modules ~~which~~ that measure time series of brightness temperatures at 26 frequencies with a sampling rate of approximately 1 Hz. The 22 GHz and the 183 GHz rotational water vapor lines are probed ~~each~~ with seven channels each along the line. In contrast to the 22 GHz module, the 183 GHz hosts a double sideband receiver~~and therefore~~, and therefore, the signal is a composite from passbands on both sides of the line. The oxygen absorption complex at 60 GHz is measured with seven single sideband channels while the double sideband receiver of the 118 GHz oxygen line has four channels. In addition, a window channel at 90 GHz is highly sensitive to liquid water emission. The noise-equivalent delta temperature (NeDT) has been determined for inflight scenes and is best for the lowest frequencies (below 0.3 K) and worst for the 90 GHz channel and 183 GHz bank (below 0.6 K). Mech et al. (2014) provide more details on instrument specifications. The receivers undergo frequent relative calibration during flight~~and therefore~~, and therefore, the most critical features of the microwave radiometer measurements is the absolute calibration (cf. Küchler et al., 2016), which is discussed further in Sect. 5.1.

3.2.2 Cloud radar

The MIRA35 cloud radar was manufactured by METEK GmbH (Elmshorn, Germany). It operates in the Ka-band at 35 GHz and is a monostatic, pulsed, magnetron, Doppler radar (Mech et al., 2014). An advantage of this frequency over the often used W-band is that it is less affected by attenuation due to condensate. Measured variables are mainly profiles of reflectivity, linear depolarization ratio, Doppler spectra and Doppler velocity. In case of the HAMP radar, measurement of Doppler velocity was strongly affected by aircraft motion and is therefore not provided. In this data set, reflectivity and linear depolarization ratio are provided. ~~Data~~ The data sampling rate is 1 Hz. At 13 km flight altitude, sensitivity is $\approx$ -30 dBZ and footprint size is $\approx$ 130 m. ~~Vertical~~ The vertical resolution of the measurements is 28.8 m. Only measurements above approximately 6 km flight altitude were conducted to avoid a too strong return from the surface into the receiver at lower levels. After some initial analyses~~a~~, an offset was discovered and quantified ~~(?)~~(Ewald et al., 2019). This correction is discussed further in Sect. 5.3.

3.2.3 Dropsondes

Vaisala RD94 dropsondes (Busen, 2012) were ~~used~~ deployed in all campaigns using the Airborne Vertical Atmospheric Profiling System (AVAPS, Hock and Franklin, 1999). Wang et al. (2015) and Vaisala (2017) report that the measurement accuracy of these sondes for pressure is 0.4 hPa, temperature is 0.2 °C and relative humidity is 2%. The accuracy of horizontal wind speed measurements is estimated to be 0.1 m s^{-1}. Overall, 525 dropsondes were released. These sondes ~~were released from the aircraft and~~ took measurements of profiles of temperature, humidity, pressure, wind speed, wind direction, and location , while falling to the surface. ~~Data~~ The data sampling rate of these sondes was usually 2 Hz. The locations for releasing the dropsondes were chosen based on the atmospheric conditions. We attempted to deploy at least one sonde in clear sky ~~condition~~ conditions to have as a reference for radiometer retrievals. For most of the flights, at least one dropsonde per flight was released. ~~Median drift length of dropsondes during their descent~~ The length of the horizontal drift distance varied substantially from drop to

drop. The median of the horizontal drift distances for all dropsonde measurements was 3.8 km~~(lower quartile 2.3, while the~~ upper and lower quartile of horizontal drift distances was 10.8 km and ~~upper quartile 10.8~~2.3 km~~).~~, respectively.

Operational constraints limited where sondes could be released. Air traffic control had to clear every release in advance. This request was only granted if the airspace below the research aircraft was empty. Therefore, it was not always possible to release the sondes ~~were~~ where it was most meaningful from a meteorological point of view. During the northern campaigns, we often had to decide to either fly below the transatlantic air traffic ~~and be able to release sondes~~ where the sondes could be released or above the traffic to get a more comprehensive profile of the entire troposphere without releasing sondes.

Another constraint for dropsondes was that the receiving unit on board the aircraft could record measurements from up to four dropsondes simultaneously. So, to launch sondes in quick succession, as was necessary for some of the NARVAL2 flights, and still record the entire lower tropospheric profile, the decision was made to fly at lower altitudes of about 8 km during flights where this was ~~necessary~~needed.

4 Data description

~~An in-depth description of the principles of HAMP radar and radiometer measurements is given in Mech et al. (2014). Here, only an example will be discussed to give an overview of how the measurements can be interpreted.~~

A combined snapshot of radar and radiometer measurements is shown in Fig. 2. The four top panels with time series of brightness temperatures T_b from different radiometer modules show integrated information of the atmosphere below the aircraft at each ~~time~~timestep. Over the radiatively cold ocean, the emission by liquid water can be seen as an increase in T_b. The strength of the emission increases with frequency and can be best seen in the window channels, at 31.4, 90 and 118 ± 8.5 GHz, (Fig. 2 (a), (c)) that are less affected by emission from water vapour and oxygen. In combination with channels sensitive to water vapor, e.g. 22 GHz (Fig. 2 (a)), the liquid water path can be derived using statistical algorithms (cf. Schnitt et al., 2017). Scattering of microwave radiation on ice particles ~~strongly~~ increases in strength considerably with increasing frequency. The strong T_b depressions in channels around 183 GHz (Fig. 2 (d)) result from scattering by larger ice particles and can be used to infer ice content. Channels along the 60 GHz oxygen complex (Fig. 2 (b)) can better penetrate the atmosphere the ~~more the~~further away they are from the absorption maximum and can ~~in this way~~therefore give information on the temperature profile. ~~Combinations of measurements from different channels can be used to derive temperature and humidity profiles, as well as liquid/snow water path.~~ In summary, the combination of measurements from different channels can be used to derive the integrated water vapor and liquid water path ~~(Schnitt et al., 2017)~~(Schnitt et al., 2017; Jacob et al., 2019), coarse resolution temperature and moisture profiles as well as information on ice and snow occurrence. An example of retrieved liquid water path and rain water path is shown in Fig. 3 to demonstrate the potential of the HAMP measurements. This scene from the NARVAL1 campaign shows the time series of the retrieved quantities together with radar reflectivity measurements. The retrieval algorithm is described in depth in Jacob et al. (2019).

The radar reflectivity (Fig. 2 (e)) shows a cross section of the clouds the aircraft passed over. Reflectivity of the cloud radar at 35 GHz is a measure of size and number of cloud droplets. The linear depolarization the ratio (LDR, Fig. 2 (f)) is defined

as the ratio of cross-polarized reflectivity factor to the co-polarized reflectivity factor. For a perfectly spherical particle, the backscattering in the cross-polarized reflectivity factor is zero in linear units and $-\infty$ in logarithmic dB units~~and thus~~, and thus, the ratio also is zero or $-\infty$, respectively. The LDR increases the more the shape of the scattering particle deviates from perfect symmetry (Oue et al., 2015). In Fig. 2 (e) and (f), the melting layer is visible as a horizontal line of high reflectivity together with high LDR values just below 1 km.

5 Quality control and data processing

Data processing has been done to convert the measured data into an easily usable format and to ensure good quality of the data. The data have been inspected and flagged accordingly. Finally, all data have been transformed onto a unified grid with a temporal resolution of 1 s. For cloud radar and dropsondes the vertical resolution is 30 m. These steps will be briefly discussed below.

5.1 Radiometer calibration

The radiometers were calibrated on the ground before almost ~~each~~ every flight using the manufacturer's warm and cold load calibration method. In this method, each radiometer was pointed successively on a warm black-body target at ambient temperature and on a cold black-body target cooled down to the boiling point of liquid nitrogen (LN_2). Targets with an open air-LN_2 interface were used during the NARVAL1 campaigns. Later, these were exchanged with targets embedded in a foam box that is transparent to microwaves, avoiding reflections at the LN_2 interface. The new targets were vertically oriented, and a metal mirror was used to redirect the view from nadir to horizontal. During flight, the radiometers were continuously calibrated using two reference loads. More details are given by Mech et al. (2014).

The quality of the original brightness temperature measurements was evaluated by comparing them with synthetic ones simulated from dropsonde profiles of clear sky. For this comparison, the sondes were filtered for clear sky conditions with low atmospheric variability, and their thermodynamic profiles were fed into the Passive and Active Microwave TRAnsfer model (PAMTRA). Random discrepancies between both can be attributed to the matching of HAMP nadir ~~measurement~~ measurements and the drifting sondes. The systematic differences could be identified~~which~~, and cannot be explained by systematic errors of the drop sonde measurement nor the microwave absorption model. Most likely they result from changes within the ~~bellypod~~ belly pod during take-off. Because some differences in the biases between different flights could be found, a bias correction based on the mean differences between synthetic and measured brightness temperatures was performed. However, for some flights only very few or no drop sondes are available. In order to arrive at a robust correction, those flights having three or less dropsondes were corrected using the campaign mean. For further information, the offset corrections used for each channel are included in the data files.

5.2 Removal of erroneous radiometer measurements

Some obvious errors in radiometer measurements occurred during the campaigns. During the NARVAL-South and NARVAL2 campaigns, the 183 GHz radiometer module suffered from instabilities during the initial phase of some flights. Because of strong drifts, the regular gain calibration (performed ~~around~~ approximately every five minutes) caused a saw tooth pattern whose amplitude ~~reduced~~ decreased with time as the module became more stable. After NARVAL2, a broken dielectric resonator oscillator (DRO) was replaced. Furthermore, ~~at some instances~~ in some instances, unreasonably high or low values were recorded by different modules likely due to instabilities in data transfer. This is also thought to be the reason that time stamps sometimes did not increase continuously but jumped ahead or backwards in time.

All data were inspected thoroughly by eye and errors of brightness temperature from saw tooth patterns or spikes in data were not corrected but removed from the data set. ~~It was attempted to reconstruct the~~ The erroneous time stamps were reconstructed where possible. If the interval with faulty time stamps was too long and reconstruction was not possible, the data have been removed. Additionally, ~~also~~ measurements during turns (roll angle $> 5°$) or when the aircraft was below 6 km altitude have been removed.

5.3 Reflectivity bias correction

By comparison with airborne and spaceborne radar measurements at 95 GHz, it has been observed that HAMP radar reflectivity ~~appeared to be~~ was too low by ~~about~~ about 8–10 dBZ. To assess the exact value of this offset, ~~?~~ Ewald et al. (2019) derived a calibration value for the HAMP cloud radar reflectivity. To this end, calibration maneuvers with constant bank angles were flown during NARVAL2 and NAWDEX while the radar emitting power was reduced to use the returned sea surface signal. Additionally, individual instrument components were measured to calibrate the cloud radar. This calibration was validated with other airborne and spaceborne measurements. ~~They~~ Ewald et al. (2019) concluded that the resulting bias of 7.6 dBZ originated from differences in software configuration and instrument calibration. This value is constant over the entire measurement range and has been added to all reflectivity measurements in this data set.

5.4 Radar data quality flag

The radar data include some features that might not be desirable to use: in the beginning of flights and sometimes also around measurement interruptions when data were recorded but no radiation was emitted, the data include noise. Further, on a couple of flights, calibration maneuvers for the radar have been executed (Sect. 5.3). During these maneuvers, the transmitting power of the radar has been changed and thus the received signal also changed. Additionally, especially when the aircraft overflew land, the unified radar data ~~contains also~~ contain pixels that are at or below the surface. All of these cases – surface and sub-surface, sea surface, noise, intervals with calibration maneuvers – have been marked in an additional data flag variable indicating the state of the radar data: data ok (0), noise (1), surface or sub-surface (2), sea surface (3), radar calibration (4). For additional information, a variable that indicates a turning of the aircraft (roll angle $> 5°$) has been added to the data set.

5.5 Temporal collocation

To ensure comparability of measurements of a certain time interval, a good temporal collocation of the instruments is needed. Temporal collocation of HAMP measurements with HALO's on-board instrumentation (BAHAMAS) has been performed independently for radar and microwave radiometers. A good synchronization with BAHAMAS lets us then assume that also radar and radiometer measurements are synchronized well.

Temporal collocation between the cloud radar and BAHAMAS has been checked by using the aircraft attitude data from BAHAMAS to correct the radar data for this attitude. The idea is that, if time stamps between both systems match perfectly, the surface return signal from the ocean surface should be a straight line, even during turns of the aircraft. To test for the time difference, the time series have been shifted and the quality of attitude correction has been assessed by looking at the variance of the height of the surface (taken as the maximum signal in each profile). The accuracy of this procedure is estimated to be 2 s. The analyzed temporal differences mainly ranged between 0 s and 2 s. The ~~maximal~~ maximum difference was 19 s. Measurements were corrected with these found offsets.

Temporal collocation between radiometer modules and BAHAMAS has been investigated by looking at the transition between land and sea. This happens shortly after take-off or before landing since both airports, Barbados Grantley Adams Airport and Keflavik Airport, are located close to the coast. This becomes possible ~~as~~ since the microwave emissivity at low frequencies strongly differs between ocean (about 0.5) and land (about 0.9). The NAVO/GHRSST global 1 km ~~land sea~~ land-sea mask (https://www.ghrsst.org/ghrsst-data-services/tools/) has been used to identify locations where the aircraft passed the shore. The footprint of the radiometers at an altitude of 900 m during take-off is approximately 70 m long, which corresponds to 0.7 s at a groundspeed of $105 \, \mathrm{m \, s^{-1}}$. The aircraft ~~is flying~~ flies with a pitch of about 11 degree~~and therefore~~, and therefore, the instruments look ahead of the aircraft position. Due to this "looking ahead" and the calculated footprint at this altitude, the accuracy of the estimated land-sea-transition is about 2.5 s. The land sea mask resolution is approximatley 0.0083°. Using this, the crossing of the shore can be determined within 3 to 12 s, depending on position (0.0083° longitude is less distance in the mid-latitudes than it is in the tropics) and aircraft speed. After a review of the measurements, all time series stayed in this interval and are ~~thus~~ therefore deemed correct.

5.6 Regridding

As mentioned in Sect. 3 and Table 5, the instruments have different sampling rates~~and in~~, and in the case of radar and dropsondes, also different vertical resolutions. To create a self-contained data set where variables from different instruments are easily comparable in time and height, the data have been transformed onto a uniform grid for each flight.

Radar measurements have additionally been corrected for aircraft attitude. After this correction, the vertical coordinate no longer ~~corresponding to range from~~ corresponds to the range from an instrument, but to height above the surface. This makes the vertical profiles of radar data from different flights comparable with each other. After that, all data have been interpolated to the new grid with 30 m vertical and 1 s temporal resolution using the nearest neighbor value. The resulting data set consists

of radar data with 1 s temporal and 30 m vertical resolution, radiometer data with 1 s temporal resolution, and dropsonde data with 30 m vertical resolution.

5.7 Filtering and gap filling

In addition to the quality control described in Sect. 5.2, spikes in dropsonde and BAHAMAS data have been filtered out. Spikes in dropsonde profiles were identified ~~as jumps in~~ if data between two measurements jumped by more than half of the data range of the entire profile. Spikes in BAHAMAS data have been identified by eye. Data gaps in dropsonde profiles have been interpolated if the gap was shorter than 10 s. With an average falling velocity of about $12\,\mathrm{m\,s^{-1}}$, this corresponds to roughly 120 m. BAHAMAS and radiometer time series have been interpolated if the gap was not longer than 3000 s (BAHAMAS) and 30 s (radiometers), which at an average aircraft velocity of $200\,\mathrm{m\,s^{-1}}$ corresponds to 6,000 km and 6 km respectively. The reasoning behind these different thresholds is that BAHAMAS data fluctuate very little in the upper troposphere/lower stratosphere. Therefore, it is reasonable to interpolate longer intervals than for radiometer data. A flag has been added to radiometer data ~~,~~ indicating which values were interpolated.

6 Data availability

The data for all flights described here ~~are~~ have been submitted to the CERA database (https://cera-www.dkrz.de/WDCC/ui/cerasearch/). The data have been released under Creative Commons Attribution-NonCommercial-ShareAlike 4.0 (CC BY-NC-SA 4.0). The data are saved as separate files for radiometer, radar, and dropsonde measurements. Radiometer and radar data sets contain auxiliary data (aircraft location and attitude). Data from each flight are saved into individual files. The data format is NetCDF (version 4).

Along with the data, quicklooks for all flights have been uploaded to the CERA database as auxiliary data. Figure 4 shows an example for one entire flight. These figures include time series of radar reflectivity, microwave radiometer brightness temperatures, aircraft attitude, and the flight track and give a quick overview of the ~~measurement~~ measurements from each flight.

The data are structured into four sets according to the four campaigns. Each set is associated with one digital object identifier: NARVAL-South (https://doi.org/10.1594/WDCC/HALO_measurements_2), NARVAL-North (https://doi.org/10.1594/WDCC/HALO_measurements_1), NARVAL2 (https://doi.org/10.1594/WDCC/HALO_measurements_3), NAWDEX (https://doi.org/10.1594/WDCC/HALO_measurements_4).

7 Summary

The HAlo Microwave Package (HAMP) was deployed on the German research aircraft HALO (High Altitude LOng range research aircraft) during four campaigns. The four campaigns took place between December 2013 and October 2016 out of Barbados and Iceland. Measured situations cover the dry and wet season over the tropical Atlantic and the cold and warm sector of mid-latitude cyclones. HAMP comprises microwave radiometers with 26 channels in the range between 20

and 183 GHz and a 35 GHz cloud radar. In sum, measurements were recorded during 295 flight hours. The flights ~~covered~~ collected data over a variety of atmospheric conditions but ~~enough of similar~~ similar enough conditions to ensure statistically representative samples. Measurements of cloud radar reflectivity and linear depolarization ratio at 35 GHz, radiometer brightness temperatures between 20 and 183 GHz and dropsonde atmospheric profiles are provided in the data set described here. Quality control has been performed to remove outliers and ensure temporal collocation of the instruments. The data ~~has~~ have been regridded onto a uniform grid for easy combined analyses. The data set has been submitted to the CERA database (https://cera-www.dkrz.de/WDCC/ui/cerasearch/, https://doi.org/10.1594/WDCC/HALO_measurements_1, https://doi.org/10.1594/WDCC/HALO_measurements_2, https://doi.org/10.1594/WDCC/HALO_measurements_3, https://doi.org/10.1594/WDCC/HALO_measurements_4) for free access. This data set adds to the relatively sparse observations of maritime clouds in the tropics and mid-latitudes. The data allow for analyses to get insight into cloud properties and atmospheric state.

Further flights with HAMP will be performed in January 2020 as part of the EUREC[4]A campaign (Bony et al., 2017) and in March 2021 as part of the HALO-(AC)[3] campaign.

References

Bony, S. and Stevens, B.: Measuring Area-Averaged Vertical Motions with Dropsondes, J. Atmos. Sci., 76, 767–783, https://doi.org/10.1175/jas-d-18-0141.1, 2019.

Bony, S., Stevens, B., Frierson, D. M. W., Jakob, C., Kageyama, M., Pincus, R., Shepherd, T. G., Sherwood, S. C., Siebesma, a. P., Sobel, A. H., Watanabe, M., and Webb, M. J.: Clouds, circulation and climate sensitivity, Nat. Geosci., 8, 261–268, https://doi.org/10.1038/ngeo2398, 2015.

Bony, S., Stevens, B., Ament, F., Bigorre, S., Chazette, P., Crewell, S., Delanoë, J., Emanuel, K., Farrell, D., Flamant, C., Gross, S., Hirsch, L., Karstensen, J., Mayer, B., Nuijens, L., Ruppert, J. H., Sandu, I., Siebesma, P., Speich, S., Szczap, F., Totems, J., Vogel, R., Wendisch, M., and Wirth, M.: EUREC4A: A Field Campaign to Elucidate the Couplings Between Clouds, Convection and Circulation, Surveys in Geophysics, 38, 1529–1568, https://doi.org/10.1007/s10712-017-9428-0, 2017.

Busen, R.: Dropsondes and Radiosondes for Atmospheric Measurements, pp. 317–329, Springer Berlin Heidelberg, Berlin, Heidelberg, https://doi.org/10.1007/978-3-642-30183-4_19, 2012.

Elsaesser, G. S., O'Dell, C. W., Lebsock, M. D., Bennartz, R., Greenwald, T. J., and Wentz, F. J.: The Multisensor Advanced Climatology of Liquid Water Path (MAC-LWP), Journal of Climate, 30, 10 193–10 210, https://doi.org/10.1175/JCLI-D-16-0902.1, 2017.

Ewald, F., Groß, S., Hagen, M., Hirsch, L., Delanoë, J., and Bauer-Pfundstein, M.: Calibration of a 35 GHz airborne cloud radar: Lessons learned and intercomparisons with 94 GHz cloud radars, Atmos. Meas. Tech., 12, 1815–1839, https://doi.org/10.5194/amt-12-1815-2019, 2019.

Hock, T. F. and Franklin, J. L.: The NCAR GPS dropwindesonde, Bull. Am. Meteorol. Soc., 80, https://doi.org/10.1175/1520-0477(1999)080<0407:TNGD>2.0.CO;2, 1999.

Houze, R. A., McMurdie, L. A., Petersen, W. A., Schwaller, M. R., Baccus, W., Lundquist, J. D., Mass, C. F., Nijssen, B., Rutledge, S. A., Hudak, D. R., Tanelli, S., Mace, G. G., Poellot, M. R., Lettenmaier, D. P., Zagrodnik, J. P., Rowe, A. K., DeHart, J. C., Madaus, L. E., Barnes, H. C., and Chandrasekar, V.: The Olympic Mountains Experiment (OLYMPEX), Bulletin of the American Meteorological Society, 98, 2167–2188, https://doi.org/10.1175/BAMS-D-16-0182.1, 2017.

Jacob, M., Ament, F., Gutleben, M., Konow, H., Mech, M., Wirth, M., and Crewell, S.: Investigating the liquid water path over the tropical Atlantic with synergistic airborne measurements, Atmos. Meas. Tech. Discuss., pp. 1–27, https://doi.org/10.5194/amt-2019-18, 2019.

Klepp, C., Ament, F., Bakan, S., Hirsch, L., and Stevens, B.: NARVAL Campaign Report, Tech. rep., Max-Planck-Institut für Meteorologie, 2014.

Krautstrunk, M. and Giez, A.: The Transition From FALCON to HALO Era Airborne Atmospheric Research, pp. 609–624, Springer Berlin Heidelberg, Berlin, Heidelberg, https://doi.org/10.1007/978-3-642-30183-4_37, 2012.

Küchler, N., Turner, D. D., Löhnert, U., and Crewell, S.: Calibrating ground-based microwave radiometers: Uncertainty and drifts, Radio Science, 51, 311–327, https://doi.org/10.1002/2015RS005826, 2016.

Mech, M., Orlandi, E., Crewell, S., Ament, F., Hirsch, L., Hagen, M., Peters, G., and Stevens, B.: HAMP â€" the microwave package on the High Altitude and LOng range research aircraft (HALO), Atmospheric Measurement Techniques, 7, 4539–4553, https://doi.org/10.5194/amt-7-4539-2014, 2014.

Oue, M., Kumjian, M. R., Lu, Y., Verlinde, J., Aydin, K., and Clothiaux, E. E.: Linear Depolarization Ratios of Columnar Ice Crystals in a Deep Precipitating System over the Arctic Observed by Zenith-Pointing Ka-Band Doppler Radar, Journal of Applied Meteorology and Climatology, 54, 1060–1068, https://doi.org/10.1175/JAMC-D-15-0012.1, 2015.

Schäfler, A., Craig, G., Wernli, H., Arbogast, P., Doyle, J. D., McTaggart-Cowan, R., Methven, J., Rivière, G., Ament, F., Boettcher, M., Bramberger, M., Cazenave, Q., Cotton, R., Crewell, S., Delanoë, J., Dörnbrack, A., Ehrlich, A., Ewald, F., Fix, A., Grams, C. M., Gray, S. L., Grob, H., Groß, S., Hagen, M., Harvey, B., Hirsch, L., Jacob, M., Kölling, T., Konow, H., Lemmerz, C., Lux, O., Magnusson, L., Mayer, B., Mech, M., Moore, R., Pelon, J., Quinting, J., Rahm, S., Rapp, M., Rautenhaus, M., Reitebuch, O., Reynolds, C. A., Sodemann, H., Spengler, T., Vaughan, G., Wendisch, M., Wirth, M., Witschas, B., Wolf, K., and Zinner, T.: The North Atlantic Waveguide and Downstream Impact Experiment, Bull. Am. Meteorol. Soc., 99, 1607–1637, https://doi.org/10.1175/BAMS-D-17-0003.1, 2018.

Schnitt, S., Orlandi, E., Mech, M., Ehrlich, A., and Crewell, S.: Characterization of Water Vapor and Clouds During the Next-Generation Aircraft Remote Sensing for Validation (NARVAL) South Studies, IEEE Journal of Selected Topics in Applied Earth Observations and Remote Sensing, 10, 3114–3124, https://doi.org/10.1109/JSTARS.2017.2687943, 2017.

Sherwood, S. C., Bony, S., and Dufresne, J. L.: Spread in model climate sensitivity traced to atmospheric convective mixing, Nature, 505, 37–42, https://doi.org/10.1038/nature12829, 2014.

Skofronick-Jackson, G. M., Johnson, B. T., and Munchak, S. J.: Detection Thresholds of Falling Snow From Satellite-Borne Active and Passive Sensors, IEEE Trans. Geoscience and Remote Sensing, 51, 4177–4189, https://doi.org/10.1109/TGRS.2012.2227763, 2013.

Stephens, G. L., Vane, D. G., Boain, R. J., Mace, G. G., Sassen, K., Wang, Z., Illingworth, A. J., O'Connor, E. J., Rossow, W. B., Durden, S. L., Miller, S. D., Austin, R. T., Benedetti, A., Mitrescu, C., and CloudSat Science Team, T.: The Cloudsat Mission And The A-Train, Bull. Am. Meteorol. Soc., 83, 1771–1790, https://doi.org/10.1175/BAMS-83-12-1771, 2002.

Stevens, B., Farrell, D., Hirsch, L., Jansen, F., Nuijens, L., Serikov, I., Brügmann, B., Forde, M., Linne, H., Lonitz, K., and Prospero, J. M.: The Barbados cloud observatory: Anchoring investigations of clouds and circulation on the edge of the itcz, Bull. Am. Meteorol. Soc., 97, 735–754, https://doi.org/10.1175/BAMS-D-14-00247.1, 2016.

Stevens, B., Ament, F., Bony, S., Crewell, S., Ewald, F., Gross, S., Hansen, A., Hirsch, L., Jacob, M., Kölling, T., Konow, H., Mayer, B., Wendisch, M., Wirth, M., Wolf, K., Bakan, S., Bauer-Pfundstein, M., Brueck, M., Delanoë, J., Ehrlich, A., Farrell, D., Forde, M., Gödde, F., Grob, H., Hagen, M., Jäkel, E., Jansen, F., Klepp, C., Klingebiel, M., Mech, M., Peters, G., Rapp, M., Wing, A. A., and Zinner, T.: A high-altitude long-range aircraft configured as a cloud observatory–the NARVAL expeditions, Bulletin of the American Meteorological Society, https://doi.org/10.1175/BAMS-D-18-0198.1, 2019.

Vaisala: Vaisala dropsonde RD94, Tech. rep., https://www.vaisala.com/sites/default/files/documents/RD94-Datasheet-B210936EN-B.pdf, 2017.

Wang, J., Young, K., Hock, T., Lauritsen, D., Behringer, D., Black, M., Black, P. G., Franklin, J., Halverson, J., Molinari, J., Nguyen, L., Reale, T., Smith, J., Sun, B., Wang, Q., and Zhang, J. A.: A long-term, high-quality, high-vertical-resolution GPS Dropsonde dataset for hurricane and other studies, Bull. Am. Meteorol. Soc., 96, 961–973, https://doi.org/10.1175/BAMS-D-13-00203.1, 2015.

Wendisch, M., Poschl, U., Andreae, M. O., MacHado, L. A., Albrecht, R., Schlager, H., Rosenfeld, D., Martin, S. T., Abdelmonem, A., Afchine, A., Araujo, A. C., Artaxo, P., Aufmhoff, H., Barbosa, H. M., Borrmann, S., Braga, R., Buchholz, B., Cecchini, M. A., Costa, A., Curtius, J., Dollner, M., Dorf, M., Dreiling, V., Ebert, V., Ehrlich, A., Ewald, F., Fisch, G., Fix, A., Frank, F., Futterer, D., Heckl, C., Heidelberg, F., Huneke, T., Jakel, E., Jarvinen, E., Jurkat, T., Kanter, S., Kastner, U., Kenntner, M., Kesselmeier, J., Klimach, T., Knecht, M., Kohl, R., Kolling, T., Kramer, M., Kruger, M., Krisna, T. C., Lavric, J. V., Longo, K., Mahnke, C., Manzi, A. O., Mayer, B., Mertes, S., Minikin, A., Molleker, S., Munch, S., Nillius, B., Pfeilsticker, K., Pohlker, C., Roiger, A., Rose, D., Rosenow, D., Sauer, D., Schnaiter,
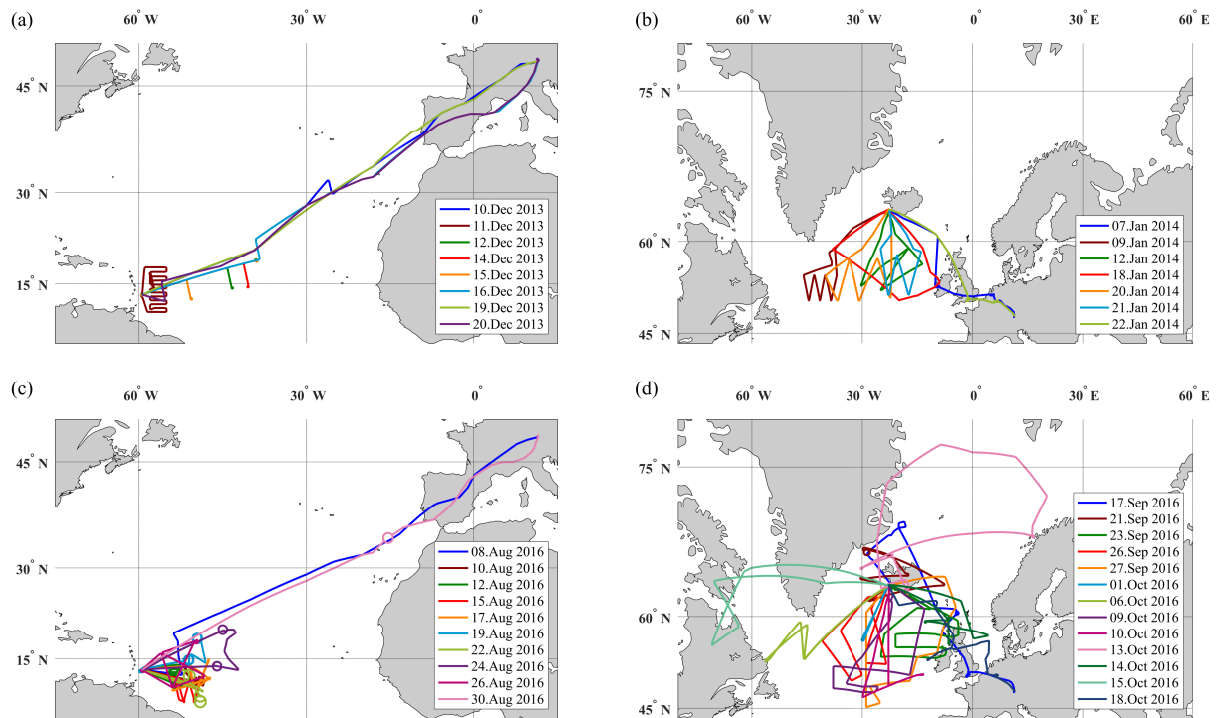
Figure 1. Flight tracks from all four campaigns: NARVAL-South (a), NARVAL-North (b), NARVAL2 (c), NAWDEX (d)

M., Schneider, J., Schulz, C., De Souza, R. A., Spanu, A., Stock, P., Vila, D., Voigt, C., Walser, A., Walter, D., Weigel, R., Weinzierl, B., Werner, F., Yamasoe, M. A., Ziereis, H., Zinner, T., and Zoger, M.: Acridicon-chuva campaign: Studying tropical deep convective clouds and precipitation over Amazonia using the New German research aircraft HALO, Bull. Am. Meteorol. Soc., 97, 1885–1908, https://doi.org/10.1175/BAMS-D-14-00255.1, 2016.

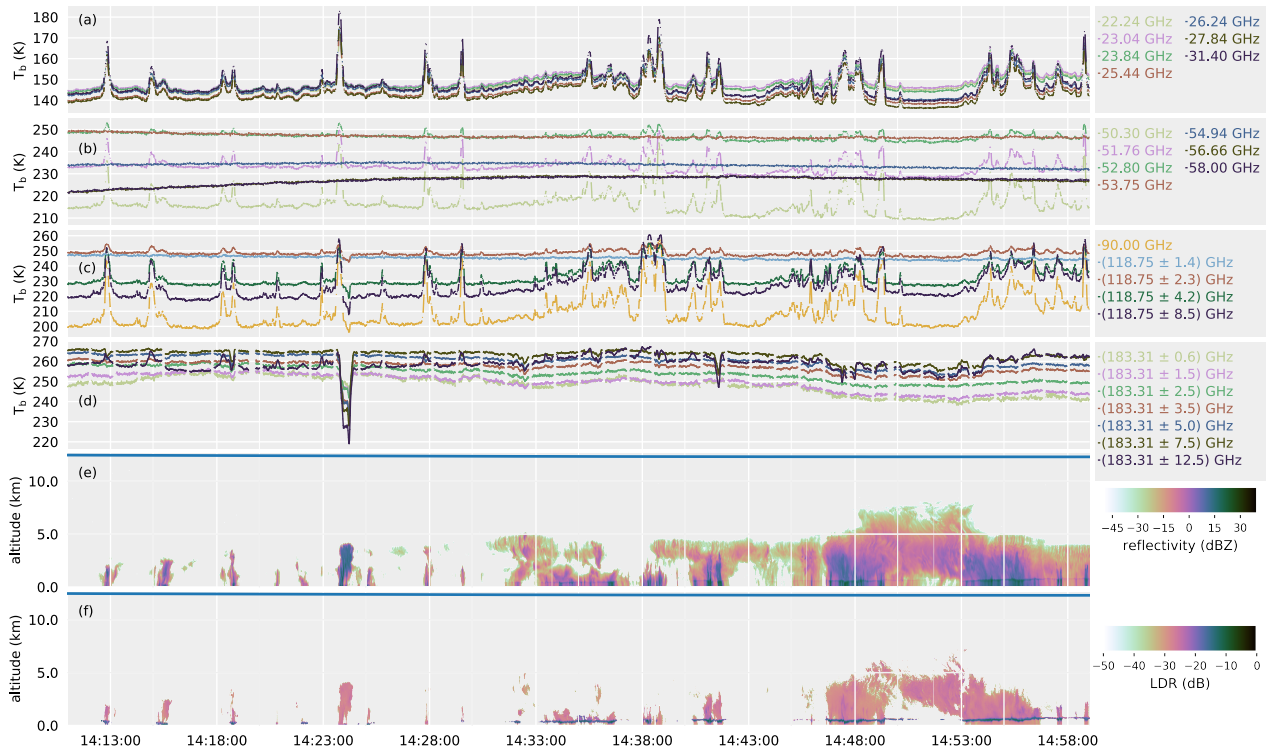**Figure 2.** Quicklook of HAMP measurements during NAWDEX flight on 06 Oct 2016. (a-d) Time series of brightness temperatures (lines) for individual radiometer modules. (e) Profiles of radar reflectivity (shaded) and HALO's flight altitude (solid line). (f) Profiles of radar linear depolarization ratio and HALO's flight altitude (solid line). The distance traveled by the aircraft during this time is roughly 710 km.
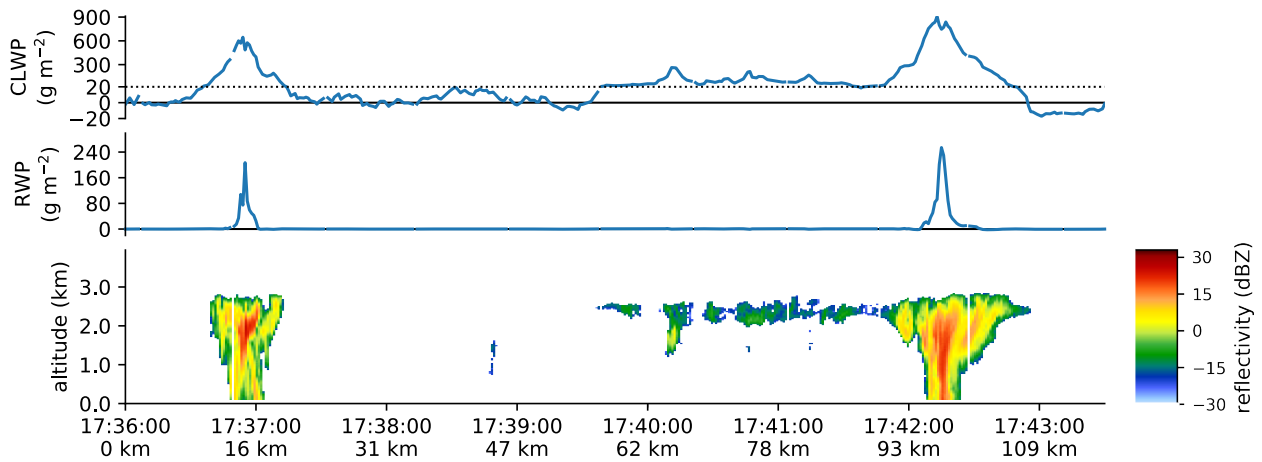
Figure 3. Example of retrieved quantities from active and passive HAMP measurements from NARVAL1 research flight 8 on December 20, 2013. Top: cloud liquid water path; middle: rain water path; bottom: radar reflectivity. Note the scale change in the top panel at $20\,\mathrm{g\,m^{-2}}$. For more information on the retrieval methods, see Jacob et al. (2019). (Figure adapted from Jacob et al. (2019))
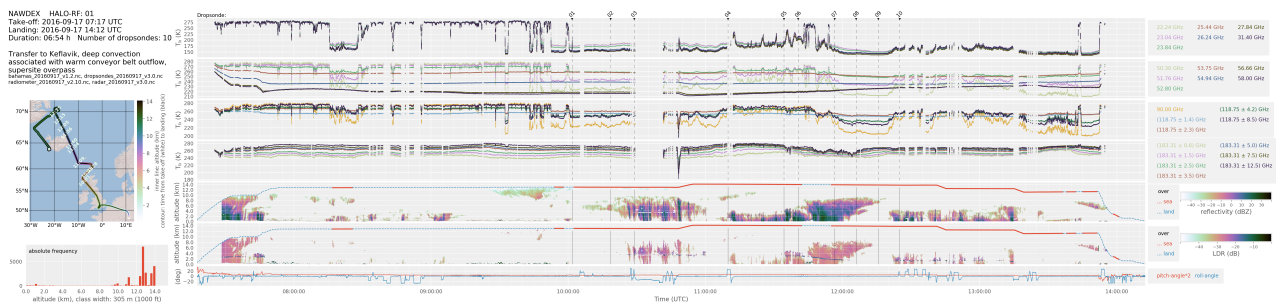
Figure 4. Example of quicklook of HAMP measurements that are available along with the data set in the CERA database. Left panel (top to bottom): flight information, flight track, altitude histogram. Center top four panels (lines): microwave radiometer brightness temperatures; fifth panel (colors): cloud radar reflectivity; sixth panel (colors): cloud radar linear depolarization ratio; bottom panel (lines): aircraft attitude. Vertical lines in center panel denote times of dropsondes released.

Table 1. List of NARVAL-South flights. All flights include observations of shallow trad wind convection. Additional flight characteristics are listed in the last column.

Date (UTC)	Start time (UTC)	End time (UTC)	Duration (hh:mm)	Number of dropsondes	Median altitude (km)	Flight characteristics
10 Dec 2013	10:13	20:41	10:27	14	12.8	~~shallow trade wind convection,~~ transatlantic cross section, A-Train overpass
11 Dec 2013	14:28	21:58	7:29	6	13.1	~~shallow trade wind convection,~~ local flight with mattress pattern, A-Train overpass[+]
12 Dec 2013	13:49	20:20	6:30	9	13.1	~~shallow trade wind convection,~~ mid-Atlantic cross section, A-Train overpass[+]
14 Dec 2013	13:35	20:21	6:45	11	13.2	~~shallow trade wind convection,~~ mid-Atlantic cross section, A-Train overpass
15 Dec 2013	15:15	21:45	6:30	9	13.2	~~shallow trade wind convection,~~ mid-Atlantic cross section, A-Train overpass
16 Dec 2013	13:10	22:59	9:48	10	13.2	~~shallow trade wind convection,~~ transatlantic cross section, A-Train overpass
19 Dec 2013	10:06	19:56	9:49	9	13.6	~~shallow trade wind convection,~~ deep convection over central Atlantic, transatlantic cross section, collocation with French Falcon
20 Dec 2013	16:30	02:32	10:02	8	13.1	~~shallow trade wind convection,~~ deep convection over central Atlantic, transatlantic cross section, A-Train overpass

[+] 183 GHz radiometer module working only part of the time

Table 2. List of NARVAL-North flights.

Date (UTC)	Start time (UTC)	End time (UTC)	Duration (hh:mm)	Number of dropsondes	Median altitude (km)	Flight characteristics
07 Jan 2014	12:07	17:49	5:42	0	12.1	transfer to Keflavik, deep convection, supersite overpasses
09 Jan 2014	08:14	17:20	9:06	11	7.3	mid level clouds in cold air outbreak, zigzag pattern, post-frontal low, A-Train overpass
12 Jan 2014	08:32	15:11	6:38	12	7.7	zigzag pattern through core and occlusion of mature mid-latitude cyclone, A-Train overpass
18 Jan 2014	08:56	14:49	5:53	5	7.9	convective development from shallow to deep in cold air behind cyclone, box pattern with altitude change, A-Train overpass
20 Jan 2014	10:16	18:45	8:29	11	7.8	convection in core of weak cyclone, zigzag pattern across system
21 Jan 2014	10:51	17:00	6:08	7	7.8	re-intensified cold air convection, zigzag pattern across system, A-Train overpass
22 Jan 2014	10:01	14:26	4:24	0	12.2	transfer from Keflavik, deep convection, Supersite overpasses

Table 3. List of NARVAL2 flights.

Date (UTC)	Start time (UTC)	End time (UTC)	Duration (hh:mm)	Number of dropsondes	Median altitude (km)	Flight characteristics
08 Aug 2016	08:13	18:51	10:38	9	14.5	transatlantic transfer, A-Train overpass[+]
10 Aug 2016	11:52	20:07	8:15	30	8.1	dry air to deep convection at the edge of the ITCZ, large circles with connecting mattress pattern, A-Train overpass[+]
12 Aug 2016	11:43	19:37	7:53	50	9.7	dry air with few shallow clouds, large circles with connecting mattress pattern[+]
15 Aug 2016	11:48	19:45	7:57	10	9.7	shallow to deep convection while crossing in and out of the ITCZ, zigzag pattern, A-Train overpass[+]
17 Aug 2016	14:48	23:07	8:19	12	14.4	shallow convection and high clouds in moist air, straight legs for satellite overpasses, collocation with A-Train, Megha-Tropiques, GPM satellites[+]
19 Aug 2016	12:29	20:52	8:23	50	9.7	partly dust laden and cloud free air, partly clearer air with shallow convection, large circles, A-Train and Megha-Tropiques overpass[+]
22 Aug 2016	13:16	20:57	7:40	13	9.7	deep convection associated with ITCZ, large circles[+]
24 Aug 2016	12:43	20:54	8:10	12	9.7	dry inflow region of hurricane Gaston (2016), deep convection at edge of hurricane, large circles and arch along hurricane[*+]
26 Aug 2016	13:43	20:54	7:10	12	9.0	Gradients of air masses: dry, shallow convection to convection in moist air, Saharan dust layer, cross pattern[*+]
30 Aug 2016	09:42	19:52	10:09	17	13.9	transatlantic transfer[*+]

[*] no radar measurements; [+] 183 GHz radiometer module working only part of the time

Table 4. List of NAWDEX flights.

Date (UTC)	Start time (UTC)	End time (UTC)	Duration (hh:mm)	Number of dropsondes	Median altitude (km)	Flight characteristics
17 Sep 2016	07:17	14:12	6:54	10	12.9	transfer to Keflavik, deep convection associated with warm conveyor belt outflow, supersite overpass
21 Sep 2016	13:55	19:25	5:29	14	12.9	deep convection associated with warm conveyor belt ascent and outflow region, legs across frontal region, GPM collocation
23 Sep 2016	07:36	16:36	9:00	21	12.0	deep convection associated with warm conveyor belt ascent and outflow region, straight legs across frontal region
26 Sep 2016	09:57	18:59	9:02	25	9.0	deep convection associated with warm conveyor belt ascent region, straight legs across cyclone center and frontal region
27 Sep 2016	11:32	20:37	9:05	20	9.0	cold air sector, strong moisture transport in warm sector, box pattern across cold and warm sector
06 Oct 2016	07:02	16:13	9:10	20	8.4	horizontal and vertical moisture gradients across a tropopause polar vortex, zigzag across moisture gradients
09 Oct 2016	10:24	19:04	8:39	1	13.3	shallow convection in cold sector, deep convection in warm conveyor belt ascent region, straight legs through warm conveyor belt
10 Oct 2016	11:58	19:37	7:38	19	8.7	warm conveyor belt ascent and outflow region, warm sector, cold sector, and core of mid-latitude cyclone, straight legs through core and frontal region of cyclone
13 Oct 2016	07:58	15:58	7:59	24	13.2	warm conveyor belt along ridge, supersite overpass, half circle around ridge from Greenland, south of Svalbard to Norway
14 Oct 2016	08:23	14:53	6:29	7	12.5	aircraft collocation with French Falcon and FAAM BAE, straight legs for aircraft collocations, A-Train overpass
15 Oct 2016	08:41	16:36	7:55	12	12.3	shallow to mid-level clouds over Labrador sea, straight legs across frontal zone, zigzag across cold air
18 Oct 2016	08:51	14:41	5:50	15	13.1	transfer from Keflavik, mid level and deep convection, supersite overpass

Table 5. Instruments used all four campaigns that provided measurements for this data set.

Name	Instrument	Measured quantities	Sampling frequency
HAMP radiometers	microwave radiometers @ K-band (22 - 31 GHz), V-band (50 - 58 GHz), W-band (90 GHz), F-band(119 GHz) and G-band (183 GHz)	brightness temperatures	$\approx$1 Hz
HAMP cloud radar	Ka band (35 GHz) pulsed magnetron radar	profiles of radar reflectivity, depol. ratio, Doppler velocity	1 Hz
dropsondes	AVAPS receiver using VAISALLA RD-94	profiles of relative humidity, temperature, horizontal wind	1 Hz
BAHAMAS[*]		aircraft attitude and location	100 Hz, 1 Hz

[*] BAHAMAS: BAsic HALO Measurement And Sensor system